

# Internal Stresses and Activation Volumes from the Stress Relaxation Behavior of Polyethylene at Large Deformations

J. KUBÁT, R. SELDÉN, and M. RIGDAHL, *Chalmers University of Technology, Dept. of Polymeric Materials, Fack S-402 20 Gothenburg, Sweden*

## Synopsis

The internal stress level in polyethylene has been determined as a function of strain by analyzing the stress relaxation behavior at room temperature. Also the influence of annealing on the magnitude of the internal stresses was studied, both with HD and LD polyethylene. The maximum initial strain was comparatively high: 20% and 40% for HDPE and LDPE, respectively. The internal stresses were found to be introduced during the initial deformation of the sample prior to the relaxation experiment. For both LDPE and HDPE the internal stress varied with the initial deformation in a manner resembling that of a stress-strain curve. In no case was a permanent residual internal stress (due to the molding process, etc.) observed. The activation volume  $v$ , evaluated from the stress relaxation kinetics, was found to be related to the effective stress  $\sigma^*$  according to  $v\sigma^* \approx 10kT$ , where  $k$  is the Boltzmann constant and  $T$  is the absolute temperature. This is in agreement with results reported earlier for both metals and polymers.

## INTRODUCTION

This paper reports on an experimental study of the stress relaxation process in high- and low-density polyethylene at comparatively high deformations, i.e., up to 20% and 40%, respectively. The upper deformation limit was chosen in order to exclude effects associated with necking phenomena. The experiments, carried out at room temperature, are a continuation of previously reported work on stress relaxation kinetics in LDPE and HDPE at deformations not exceeding 1.5%.<sup>1</sup> In both cases the results are analyzed using the idea of stress-aided thermal activation, a method commonly used in describing flow in metals and other crystalline solids.<sup>2,3</sup>

The dependence of the activation volume on the effective stress will be shown to be largely similar to the dependence observed earlier at low deformations.<sup>1</sup> (The activation volume concept used here is sometimes termed "activation strain volume" or "stress activation volume" to avoid confusion with the activation volume determining the flow rate due to change in the applied hydrostatic pressure.) Also the role played by the internal stress, both permanent and strain induced, as a rate-determining factor remains unchanged when the deformation of the samples is increased to 20% and 40% for HDPE and LDPE, respectively. Of special interest are the quantitative similarities between flow in polyethylene and other classes of solids, e.g., metals, demonstrated by a generally valid dependence between the activation volume and the effective stress. It may be concluded that the idea of stress-aided thermal activation in its present form cannot provide a satisfactory description of relaxational flow in solids.

## THEORETICAL BACKGROUND

It is known that flow in solids at high stresses and/or low temperatures follows the exponential law of flow, eq. (1), while at lower stresses and/or high temperatures a power-type law is applicable, eq. (2). With regard to creep, the distinction between high and low stresses is obvious; for stress relaxation, it is relative only in that the first part (shorter times) always obeys eq. (1), while eq. (2) applies at longer times (lower stresses). The two formulae are normally written as follows:

$$\dot{\sigma} = -A \exp(v\sigma^*/kT) \quad (\text{exponential law}) \quad (1)$$

$$\dot{\sigma} = -B(\sigma^*)^n \quad (\text{power law}) \quad (2)$$

Equation (1) stems from the concept of stress-aided thermal activation,<sup>1,4,5</sup> and eq. (2) is based on observations of the stress dependence of the dislocation velocity<sup>6</sup>;  $A$ ,  $B$ , and  $n$  in eqs. (1) and (2) are assumed to be independent of stress,  $k$  is Boltzmann's constant,  $T$  is the temperature, and  $v$  denotes the activation volume, which is given from eq. (1) as<sup>7</sup>

$$v = kT \left( \frac{\partial \ln \dot{\sigma}}{\partial \sigma^*} \right)_{T,p} \quad (3)$$

where  $p$  is the applied hydrostatic pressure; actually eqs. (1) and (3) presuppose that the activation energy decreases linearly with stress.<sup>8</sup> The stress used in eqs. (1)–(3) is the effective stress  $\sigma^*$ , i.e. the difference between the applied  $\sigma$  and the internal stress  $\sigma_i$ .

If eq. (3) is applied to the power-law region of the stress relaxation curve, one obtains<sup>7</sup>

$$v = nkT/\sigma^* \quad (4)$$

It is also known<sup>7,9</sup> that for the exponential law eq. (1), being equivalent to a linear  $\sigma(\log t)$  plot with slope  $F$ ,  $v$  is given by

$$v = kT/F \quad (5)$$

For a wide variety of material with different structures and compositions we found that<sup>9</sup>

$$F = (0.1 \pm 0.01)\sigma_0^* \quad \text{if } F = \left( -\frac{\partial \sigma}{\partial \ln t} \right)_{\max} \quad (6)$$

where  $\sigma_0$  denotes the initial stress of the experiment. The linear region of the relaxation curve with the maximum slope  $F$  normally extends over a few decades of time. Equations (5) and (6) now give

$$v\sigma_0^* = 10kT \quad (7)$$

for the exponential-law region of the relaxation curve.

A more detailed account of the theoretical background can be found in earlier papers<sup>1,10</sup> containing, among other things, a discussion of the stress level demarcating the range of validity of eqs. (1) and (2). It may suffice here to mention that the stress denoting the transition from exponential to power law flow,  $\sigma_{tr}$ , is given by the following expression:

$$\sigma_{tr}^* \approx \frac{n}{10} \sigma_0^* \quad (8)$$

## EXPERIMENTAL

### Samples

The following grades of polyethylene were used: HDPE—Lupolen 6011L (BASF), density  $0.963 \text{ g/cm}^3$ , melt index  $4.0\text{--}6.0 \text{ g/10 min}$  (MFI 190/2); annealed density  $0.982 \text{ g/cm}^3$ . LDPE—Lupolen 1810D (BASF), density  $0.921 \text{ g/cm}^3$ , melt index  $0.1\text{--}0.3 \text{ g/10 min}$  (MFI 190/2); annealed density  $0.922 \text{ g/cm}^3$ .

Samples of HDPE and LDPE (dimensions  $0.5 \times 5 \times 50 \text{ mm}$ ) were produced by compression molding ( $165^\circ\text{C}$ ,  $0.5 \text{ MPA}$ ,  $3 \text{ hr}$ ). Some of the specimens were annealed for  $36 \text{ hr}$  (HDPE at  $120^\circ\text{C}$ , LDPE at  $80^\circ\text{C}$ ). Measurements with a differential scanning calorimeter (Perkin-Elmer DSC 2) gave the following melting points: HDPE—unannealed  $133^\circ\text{C}$ , annealed  $135^\circ\text{C}$ ; LDPE— $110^\circ\text{C}$  both annealed and untreated. The heating rate was  $20^\circ\text{K/min}$  for all specimens.

### Method

The relaxometer used has been described earlier.<sup>9</sup> The temperature of measurement was  $20^\circ \pm 0.1^\circ\text{C}$  and the strain rate,  $1.4 \times 10^{-2} \text{ sec}^{-1}$ . The maximum deformation was 20% for unannealed and 10% for annealed HDPE; for LDPE the corresponding strain was 40% for both types of material. In no case was the deformation large enough to cause necking.

## RESULTS

### Stress-Strain Curves

In Figure 1, the stress-strain curves for annealed and untreated HDPE are displayed in terms of engineering (nominal) and true variables. Figure 2 shows the corresponding results for LDPE. Evidently, the annealing resulted in an increase of the modulus and yield stress. For HDPE, the cold-drawing ability was lost, the samples breaking in a brittle manner.

### Stress Relaxation

Some typical examples of stress relaxation curves obtained with LDPE and HDPE at various initial deformations are shown in Figure 3. Increasing the initial deformation shifted the curves for LDPE toward longer times, eq. (1) being valid up to  $100 \text{ sec}$ . At lower deformations (less than 1.5%) the exponential law was not valid for times longer than  $30 \text{ sec}$ . Increasing the initial strain thus shifts the transition between the exponential and power-law regions toward longer times. For HDPE the opposite applied, an increase in strain shifted the transition to somewhat shorter times ( $15\text{--}20 \text{ sec}$ ).

From eqs. (1) and (2) it follows that  $\log \dot{\sigma}$  versus  $\log t$  should consist of two linear portions with slope  $-1$  in the exponential region and  $-n/(n-1)$  in the power-law region.<sup>11</sup> Figure 4 gives a few examples of such plots. These support the assumption made above that a relaxation curve can be divided into two regions obeying eqs. (1) and (2), respectively. Furthermore, the experimentally determined transition stress,  $\sigma_{tr}$ , is in accordance with what is to be expected from eq. (8).

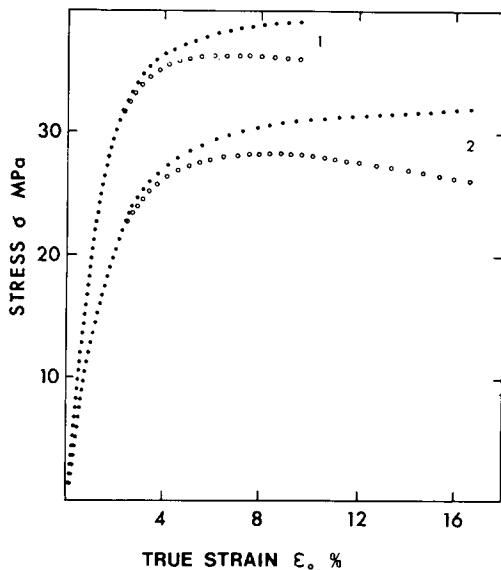


Fig. 1. Stress-strain curves for HDPE displayed as nominal (O) and true (●) values of stress vs true strain: (1) annealed; (2) nonannealed.

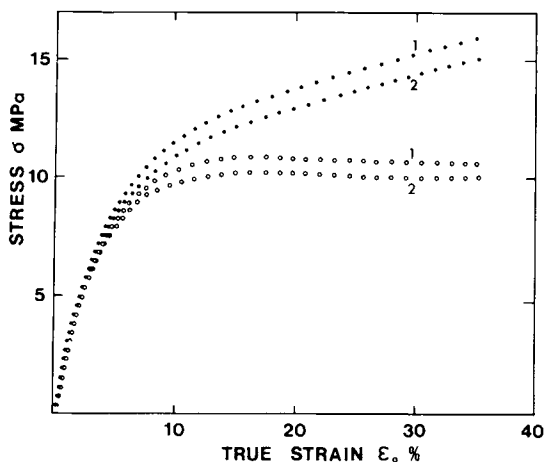


Fig. 2. Stress-strain curves for LDPE displayed as nominal (O) and true (●) values of stress vs true strain: (1) annealed; (2) nonannealed.

### Internal Stresses

In order to determine the effective stress which, according to accepted knowledge, governs the stress relaxation kinetics, the internal stress has to be evaluated. In the present case, as in the earlier paper<sup>1</sup>, the stress relaxation method proposed by Li<sup>12</sup> was employed. According to this,  $-d\sigma/d \log t$  is plotted versus  $\sigma$  and the intercept of the resulting line with the  $\sigma$ -axis is taken as a measure of  $\sigma_i$ . In general, this total internal stress could contain both permanent (frozen-in),  $\sigma_{ir}$ , and strain-dependent internal stress contributions,  $\sigma_{id}$ .<sup>1</sup> The strain-independent component can be isolated as follows: the slope  $F$  is plotted versus the initial stress  $\sigma_0$ , and the intercept of this straight line, and the  $\sigma_0$ -axis provides a measure of  $\sigma_{ir}$ .<sup>5</sup>

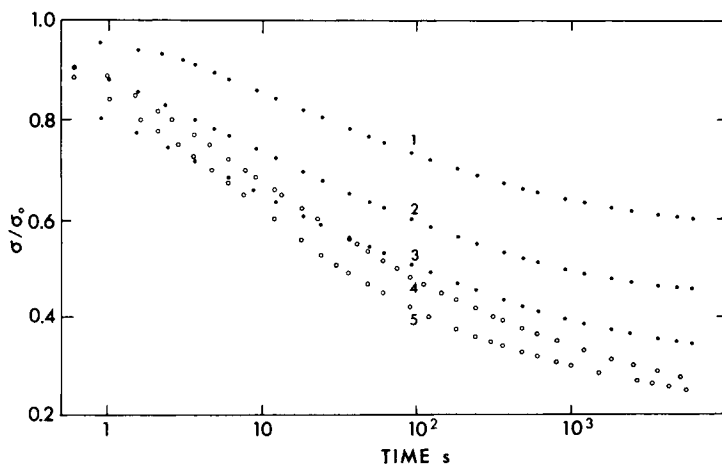


Fig. 3. Stress relaxation curves for LDPE (●) and HDPE (○) as  $\sigma/\sigma_0$  vs  $\log t$  plots at various deformations: (1)  $\epsilon_0 = 29.3\%$ ; (2)  $\epsilon_0 = 2.3\%$ ; (3)  $\epsilon_0 = 0.5\%$ ; (4)  $\epsilon_0 = 1.5\%$ ; (5)  $\epsilon_0 = 9.6\%$ .

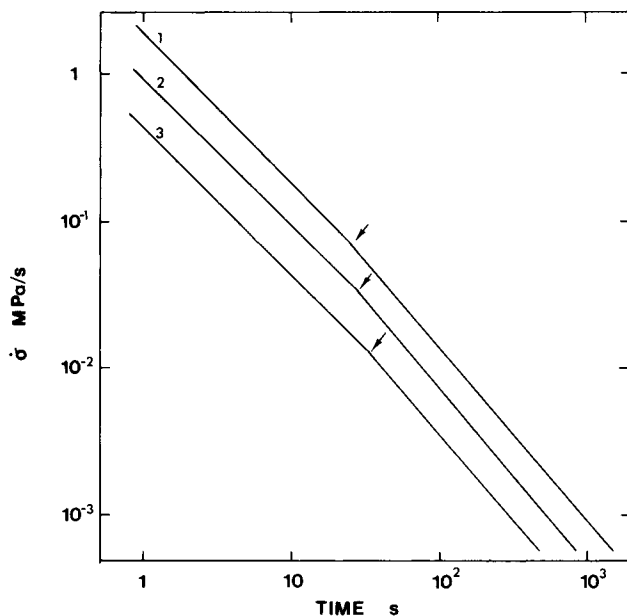


Fig. 4. Relation between flow rate and time for HDPE at  $\sigma_0 = 20.3, 10.2, 5.0$  MPa, respectively. Arrows indicate the transition between the exponential and the power law of flow: (1)  $\sigma_0 = 20.3$  MPa; (2)  $\sigma_0 = 10.2$  MPa; (3)  $\sigma_0 = 5.0$  MPa.

The variation of the total internal stress  $\sigma_i$  with strain is shown for LDPE in Figure 5. As can be seen, the increase of the total  $\sigma_i$  level with the initial strain  $\epsilon_0$  can be described by two straight lines, one at lower deformations  $\epsilon_0 < 5.5\%$ , and shows the linear increase of  $\sigma_i$  with  $\epsilon_0$  in this range. At  $\epsilon_0 > 5.5\%$  the slope becomes smaller. With HDPE, similar results were obtained even though the experimental scatter was greater here. There is, however, a change in slope at  $\epsilon_0 \approx 4.5\%$  (Fig. 6).

Qualitatively, the way in which  $\sigma_i$  increases with  $\epsilon_0$  is reminiscent of the shape of the stress-strain curve of PE, a material with a pronounced plastic flow region.

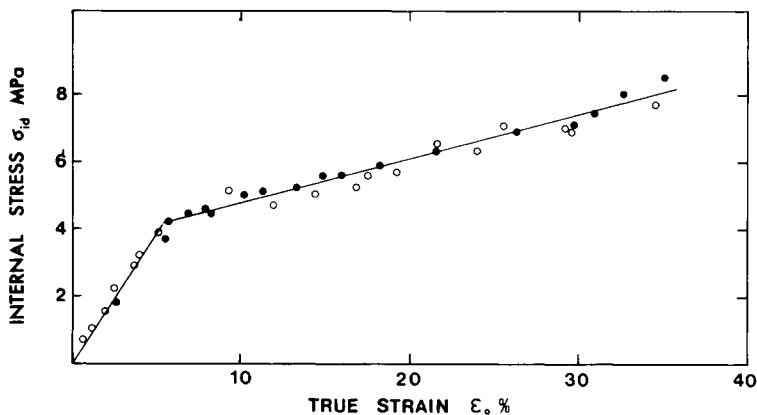


Fig. 5. Variation of true internal stress with the true strain for LDPE: (O) nonannealed; (●) annealed.

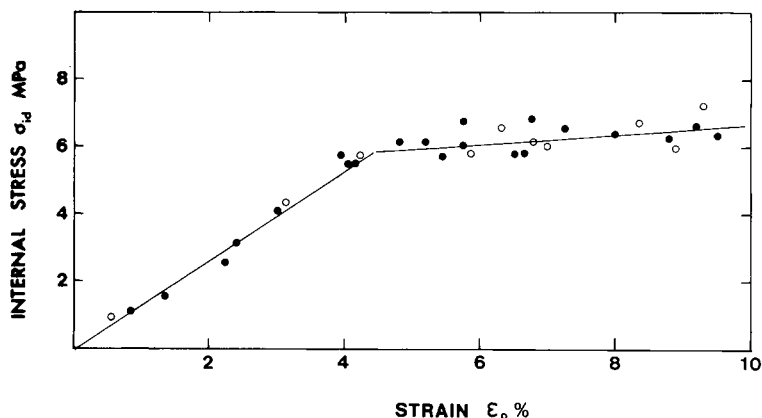


Fig. 6. Variation of true internal stress with the true strain for HDPE: (O) nonannealed; (●) annealed.

It is, therefore, surprising to find that, despite the rather large differences in the shape of the stress-strain curves of LDPE and HDPE, respectively, the corresponding  $\sigma_i$ - $\epsilon$  curves, as shown in Figures 5 and 6, are largely similar.

For  $\epsilon_0$  values in excess of ca. 5%, the ratio  $\sigma_i/\sigma_0$  for LDPE changed very little (from 0.45 to 0.50). Annealing was without influence. For HDPE, the  $\sigma_i/\sigma_0$  ratio at initial strains larger than ca. was 0.15–0.18 for the annealed and 0.20–0.23 for the untreated samples.

From the results reproduced in Figures 5 and 6 it seems fair to conclude that the total internal stress level  $\sigma_i$  largely consists of internal stresses introduced into the sample during the straining procedure preceding the actual relaxation measurement. The conclusion that possible permanent stresses  $\sigma_{ir}$ , originating from the molding operation, are absent is also directly evidenced by the position of the  $F$ - $\sigma_0$  lines, these lines going through the origin for all the samples investigated here. This is shown in Figure 7 for annealed HDPE. However, it is important to note that the slope of this curve increases when the applied stress (strain) exceeds a critical value which approximately corresponds to the tensile strength at yield. The corresponding strain obtained from the stress-strain

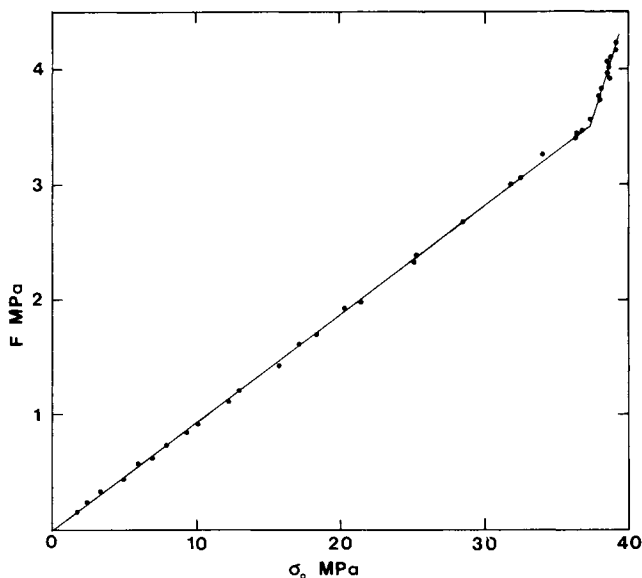


Fig. 7. Maximum slope  $F$ , defined as  $(-d\sigma/d \ln t)_{\max}$  vs  $\sigma_0$  for annealed HDPE.

diagram is approximately 6%. A similar behavior has also been observed for b.c.c. metals by Feltham and Hawkins.<sup>13</sup> For LDPE, on the other hand, the same could not be observed.

### The $F(\sigma_0^*)$ Ratio and the Activation Volume

The ratio  $F/\sigma_0^*$  of the slope of the rectilinear  $\sigma$ -versus- $\log t$  region of the stress relaxation curves and the effective initial stress has been shown previously to assume the value  $0.1 \pm 0.01$ , independent of the nature of the solid investigated and largely also of the experimental conditions.<sup>9</sup>

Stress relaxation results for polyethylene at low deformations were in good agreement with this finding.<sup>1</sup> The present measurements provide further support for the general validity of Eq. (6), this time with a semicrystalline polymer deformed to appreciable strains. Even though the  $F/\sigma_0^*$  ratio was slightly higher (0.10–0.12) in this case increasing with strain for both LDPE and HDPE, it still can be said that the results obtained fit well into the general pattern.

The slightly higher values  $F/\sigma_0^*$  found here are possibly to be expected for experiments where the straining times involved are long, rather than being dependent on the actual value of the deformation. An increase in the value of the relative slope  $F/\sigma_0^*$  with straining time follows rather naturally from the assumption of a relaxation time spectrum, the relaxation taking place during the straining operation narrowing the width of the original, unperturbed spectrum. The idea of stress-aided activation does not offer such an explanation.

### The Power-Law Exponent $n$

Numerous investigations on metals have demonstrated that the value of  $n$ , the power-law exponent in eq. (2), is subject to an appreciable scatter.<sup>14</sup> For metals,  $n$  values between 6 and 12 are normally found.<sup>3</sup> The data given in Figure

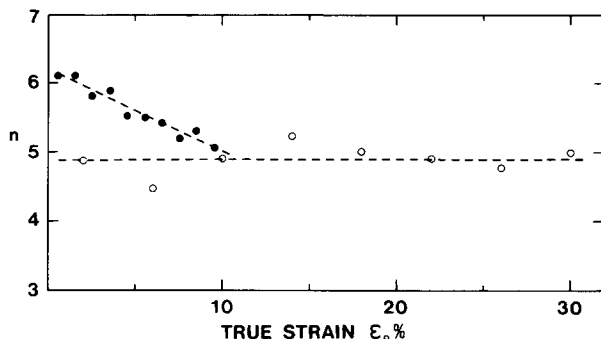


Fig. 8. Variation of the power-law exponent  $n$  vs initial strain  $\epsilon_0$  for HDPE (●) and LDPE (○). Each point represents an average  $n$  value for strain interval of 1% for HDPE and 4% for LDPE.

8 show that the power-law flow of LDPE is characterized by  $n = 5 \pm 1$ , independent of strain. With HDPE,  $n$  changes slightly from 6–7 at low strains to about 5 at higher values.

## DISCUSSION

With respect to the parameters under study, the stress relaxation behavior of LD and HDPE in the region of large deformations appears to follow closely the pattern observed earlier at deformations not exceeding 1.5%. In the present case the upper limit of the deformations studied was set by the necking tendency of the samples.

It is interesting that the comparatively high initial strains used did not influence the basic character of the internal stress pattern. As shown by direct measurement, all the samples used were free from permanent internal stresses  $\sigma_{ir}$ , i.e., stresses normally frozen in during the preparation of the sample. The internal stress level, determined using Li's method,<sup>12</sup> was thus entirely due to the stress  $\sigma_{id}$ , introduced into the samples during the straining operation. As has been found at low  $\epsilon_0$  values, the variation of  $\sigma_{id}$  with initial strain was reminiscent of the course of the stress-strain curves, even though the difference between LDPE and HDPE with regard to  $\sigma_{id}-\epsilon_0$  was rather small.

According to the basic idea regarding the role of the effective stress as a flow rate-determining factor, one could expect that a sample free from permanent internal stresses would relax to  $\sigma_\infty = 0$ ,  $\sigma_\infty$  being the stress at infinite time. Our results show that such an assumption is incorrect. Instead,  $\sigma_\infty$  will assume a value equal to  $\sigma_{id}$ , the internal stress contribution caused by deforming the sample prior to the relaxation experiments. Needless to say,  $\sigma_{id}$  will also influence the entire course of the relaxation curve, since the effective stress  $\sigma^*$  is equal to  $\sigma - \sigma_{id}$ , which also applies to samples free from internal stresses in the usual meaning of the word.

The division of the total  $\sigma_i$  value into the contributions of  $\sigma_{id}$  and  $\sigma_{ir}$  is, in view of these facts, of obvious importance for understanding the mechanisms of flow in solid materials. The fact that no attention appears to have been paid to this has a rather simple explanation. In metals, the  $\sigma_{ir}$  contribution is normally very large in comparison with the  $\sigma_{id}$  values that can be induced by deforming the sample. In normal metallic materials  $\sigma_{id}$  is thus of minor importance only. In contrast to this, the  $\sigma_{id}/\sigma_{ir}$  balance in polymers is different. As exemplified



above,  $\sigma_{ir}$  may be zero, at the same time as  $\sigma_{id}$  may assume significant values. To account for the fact that the role of the  $\sigma_{id}$  contribution has not been considered earlier, it may suffice here to mention that studies of  $\sigma_i$ -flow rate relationships are as rare in the polymer area as they are frequent in the field of metallic materials.

The permanent internal stress  $\sigma_{ir}$  can assume high values also in certain polymeric systems. In the first place, this is the case with highly oriented polymers.<sup>15</sup> In such samples, the  $\sigma_{ir}$  contribution normally overshadows the strain-induced part of the total  $\sigma_i$  level. It may be noted that effects of this type did not occur in the strain range used in the present work.

The mother major finding of this paper is the confirmation of the validity of eq. (6) for polyethylene deformed to rather high strains. In view of the considerable experimental support of this equation gathered with different solids elsewhere,<sup>9,10</sup> this is hardly surprising. It may only be added here that the representation of the results in terms of an activation volume and its dependence on the effective stress should not be taken too literally. It is difficult to reconcile the idea of an activation volume depending only on  $\sigma^*$ , be it for rubber or for steel, with normal structural concepts. Instead, the results described above call for a modification of eq. (1) in the following way:

$$\dot{\sigma} \approx \exp(\alpha\sigma^*/\sigma_0^*) \quad (9)$$

where  $\alpha$  is a parameter depending on the number of units taking part in the relaxational flow process. A detailed discussion of these problems can be found elsewhere.<sup>10,16</sup>

The authors wish to thank Miss Annette Jonasson for skillful experimental assistance. Thanks are also due to the Swedish Board for Technical Development and to the Swedish Polymer Research Foundation for financial support.

## References

1. J. Kubát, M. Rigdahl, and R. Seldén, *J. Appl. Polym. Sci.*, **20**, 2799 (1976).
2. N. Balasubramanian and J. C. M. Li, *J. Mater. Sci.*, **5**, 434 (1970).
3. F. Garofalo, *Fundamentals of Creep and Creep Rupture*, Macmillan, New York, 1965, p. 91.
4. O. D. Sherby and J. E. Dorn, *J. Mech. Phys. Sol.*, **6**, 145 (1958).
5. J. Kubát and M. Rigdahl, *Int. J. Polym. Mater.*, **3**, 287 (1975).
6. W. G. Johnston and J. J. Gilman, *J. Appl. Phys.*, **30**, 129 (1959).
7. R. de Batist and A. Callens, *Phys. Stat. Sol. (a)*, **21**, 591 (1974).
8. H. Eyring, *J. Chem. Phys.*, **4**, 283 (1936).
9. J. Kubát, D.Sc. Thesis, Stockholm University, Stockholm, Sweden, 1965.
10. J. Kubát and M. Rigdahl, *Mater. Sci. Eng.*, **24**, 223 (1976).
11. R. de Batist, *Rev. Def. Behav. Mater.*, **1**, 71 (1975).
12. J. C. M. Li, *Can. J. Phys.*, **45**, 493 (1967).
13. P. Feltham and A. Hawkins, *Mater. Sci. Eng.*, **17**, 239 (1975).
14. N. Balasubramanian, J. C. M. Li, and M. Gensamer, *Mater. Sci. Eng.*, **14**, 37 (1975).
15. J. Kubát, J. Petermann, and M. Rigdahl, *Mater. Sci. Eng.*, **19**, 185 (1975).
16. G. Grimwall, J. Kubát, and M. Rigdahl, in *Proc. VIIth Int. Congr. on Rheology*, C. Klason and J. Kubát, Eds., Gothenburg, 1976, p. 234.

Received October 26, 1976

Revised April 4, 1977